Characterization of Star Adhesive Sealants Based On PEG/Dextran Hydrogels

Natalie Artzi,* Tarek Shazly, Cristina Crespo, Adriana Bon Ramos, H. Keith Chenault, Elazer R. Edelman

Swellable PEG amine/dextran aldehyde composite materials are emerging as a controlled, biocompatible tissue adhesive. We explain how preservation of natural tissue amines provides biocompatibility for PEG/dextran that exceeds the stringent, destructive cyanide-based chemistry of cyanoacrylates, and adhere far better than fibrin glue. Strategic variations of material composition allow for the improvement of biocompatibility and adhesion strength. Material variations can be tailored to match the needs of specific tissue beds for an array of clinical applications. PEG/dextran cohesive properties are most responsive to variations in the PEG component (number of arms and solid content), while tissue/material adhesion strength is primarily determined by the number of aldehydes in the dextran.

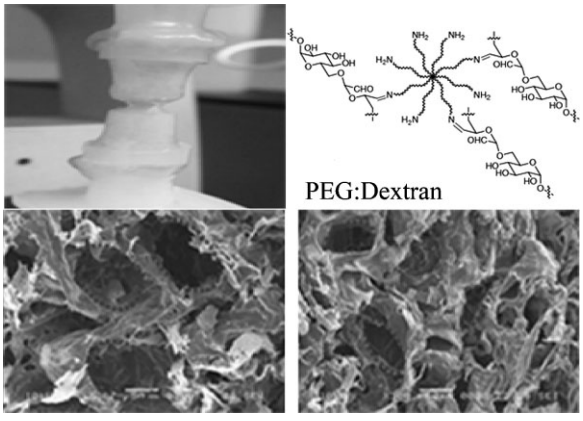

Introduction

Adhesive biomaterials[1,2] are used increasingly to reinforce anastomotic integrity between tubular structures, repair surface lacerations and abrasions, and/or fill void spaces following tissue resection procedures. Commercially available sealants are limited by inadequate adhesion and/or biocompatibility.[1,3–5] Fibrin glue contains an antiproteinase, which impairs the ingrowth of vascular granulation tissue and healing of surgical anastomoses.[6] Insufficient adhesion to tissue was evident when fibrin sealant was applied to the liver. There were no clinical benefits with respect to blood loss, transfusion requirement, incidence of biliary fistula, or overall outcome.[7] Cyanoacrylate-based materials are cytotoxic, harmful to tissues,[8] and even dangerous to medical staff who are instructed to avoid direct contact with the compound.[9]

Aldehydes have long been used for tissue crosslinking and were proposed recently for use as adhesive sealants.[2] Glutaraldehyde and formaldehyde are classic tissue preservatives which interdigitate within tissues and react chemically with tissue proteins.[10] Aldehyde groups presented on these short carbon backbones create highly crosslinked tissue structures but do so while limiting their biocompatibility and potential for non-fixative applications.[11–13]

N. Artzi, T. Shazly, C. Crespo, A. B. Ramos, E. R. Edelman
Harvard-MIT Division of Health Sciences and Technology, Massachusetts Institute of Technology, Cambridge, Massachusetts 02139, USA
Fax: +1 617 253 2514; E-mail: nartzi@mit.edu
C. Crespo, A. B. Ramos
Institut Quiimic de Sarrià, Universitat Ramon Llull, Barcelona 08017, Spain
H. K. Chenault
Biochemical Sciences and Engineering, Central Research and Development, DuPont Experimental Station, Wilmington, DE19880, USA
E. R. Edelman
Cardiovascular Division, Department of Medicine, Brigham and Women's Hospital, Harvard Medical School, Boston, Massachusetts 02115, USA

Macromol. Biosci. **2009**, *9*, 754–765

DOI: 10.1002/mabi.200800355

We propose that the toxicity following aldehyde-tissue interactions could be reduced if the aldehydes are mounted on higher molecular weight materials such as dextran, a natural polymer of glucose residues.[14] This natural polymer is hydrophilic, biocompatible and non-toxic,[15] which can be prepared in a variety of molecular masses.[16] By combining dextran aldehyde polymers with an aminated PEG, one can form a gel that can be applied to tissues and cured in situ.[14] PEG hydrogels are readily functionalized, nontoxic, non-immunogenic, blood-compatible, and FDA approved for various clinical uses. PEG has already been used for a wide range of applications such as tissue regeneration,[17] drug delivery,[18] coating,[19] and postoperative adhesions prevention.[20] PEG was successfully utilized as an anchor for the incorporation of 3,4-dihydroxyphenylalanine (DOPA) residues to impart wet-adhesive and curing properties.[21] Although not biodegradable, low molecular weights PEG-polymers (up to 10 kDa) form nontoxic metabolites that can be readily excreted from the body.[22]

We postulate that bioeliminable PEG/dextran material systems consisting of a core dextran polymer crosslinked to relatively short PEG polymers can serve as a better alternative to high molecular weight PEG or dextran homopolymers. PEG/dextran cytotoxicity to fibroblasts was qualitatively assessed and was generally non-toxic. The inflammatory potential of PEG/dextran was evaluated by exposing J774 macrophage cells to crosslinked adhesives, and measuring TNF-α release from macrophages. PEG/dextran tissue adhesive did not elicit inflammatory TNF-α release from macrophages, which suggests that this tissue adhesive is non-cytotoxic and non-inflammatory.[23] In addition, PEG/dextran adhesive was successful in sealing small intestinal puncture and corneal incisions to pressures higher than 100 and 500 mm Hg,[24] respectively, and was non-cytotoxic to bovine corneal endothelial cells.[25]

The existing limitations of commercially available materials have highlighted the need for an alternative adhesive system with tunable adhesion and bioreactivity. This paper demonstrates the complexity in the development of an adhesive that will provide a node for modulated adhesion while maintaining biocompatibility, conferring controllable mechanical properties and degradation kinetics. We believe that only a system that encompasses flexible design parameters, as in the case of PEG and dextran, can fulfill the necessary requirements an adhesive material should meet, and ultimately overcome existing limitations in sealant technology. The PEG/dextran sealant's performance was evaluated based on gelation time, swelling and degradation kinetics, stiffness, adhesion strength, and biocompatibility. This sealant overcomes the existing limitations in sealant technology.

Experimental Part

Dextran Aldehyde Synthesis

Oxidized dextrans, also referred to as dextran aldehydes, were a gift from E. I. DuPont de Nemours & Co, Inc and were prepared with ≈20 or 50% aldehyde content conversion from dextrans having an average molecular weight of 10, 40, or 60 kDa (Sigma).

Dextran Oxidation

Dextran oxidation reaction is described for dextran having average molecular weight of 10 kDa, and the same protocol applies to other molecular weight dextrans. Dextran (19.0 g; 0.12 mol saccharide rings; average molecular weight 8 500–11 500; Sigma no. D9260) was added to 170 g of distilled water in a 500 mL round bottom flask. The mixture was stirred for 15 to 30 min to produce a solution; then a solution of 17.7 g (0.083 mol; $\overline{M}_w = 213.9$) sodium periodate (Sigma) in 160 g of distilled water was added to the dextran solution. The mixture was stirred at room temperature for 5 h. At the end of 5 h, the solution was removed from the round bottom flask, divided into four equal volumes and dispensed into four dialysis membrane tubes (molecular-weight cutoff 3 500 Da). The tubes were dialyzed in deionized water for 4 d; the water was changed twice daily during this time. The aqueous solutions were removed from the dialysis tubes, then frozen using liquid nitrogen, and lyophilized to afford white, fluffy oxidized dextran. Other aldehyde conversions were obtained by varying the concentration of the periodate solution used.

Determination of Dialdehyde Content

The oxidized dextran (0.1250 g) was added to 10 mL of 0.25 M NaOH in a 250 mL Erlenmeyer flask.[26] The mixture was gently swirled and then placed in a temperature-controlled sonicator bath at 40 °C for 5 min until all the material dissolved. The sample was removed from the bath and the flask was cooled under cold tap water for 5 min. 15 mL of 0.25 M HCl was added to the solution, followed by the addition of 50 mL distilled water and 1 mL of 0.2% phenolphthalein solution. This solution was titrated with 0.25 M NaOH to an endpoint determined by a color change from yellow to purple/violet. The same titration was carried out on a sample of the starting dextran to afford background aldehyde content. The dialdehyde content, also referred to as oxidation conversion or degree of oxidation, in the oxidized dextran sample was calculated according to

$$\text{Dialdehyde content} = \left[\frac{(N_b - N_a)_s}{W_s/M}\,\frac{(N_b - N_a)_p}{W_p/M}\right] \times 100\% \qquad (1)$$

where N_b is the total amount (equiv.) of base, N_a the total amount of acid, W the dry sample weight (mg), and M the weight-average molecular weight of the polysaccharide repeat unit (= 162 for dextran), and the indices s and p denote the oxidized and original sample, respectively.

Typically, three determinations were done and the degree of oxidation given is the mean of the three determinations.

PEG-Amine Synthesis

A linear PEG of 2 kDa (Sigma) or 8-arm PEG of 10 kDa (each arm 1 250 Da) (NOF America Corporation, White Plains, NY, USA) was used as substrates to form linear PEG-amine or 8-arm PEG-amine. The reactions are similar and we will detail in here the 8-arm PEG octaamine synthesis which was done using a two-step procedure.[14] In the first step, the 8-arm PEG 10 kDa was converted to an 8-arm PEG 10 kDa chloride by reaction with thionyl chloride (Figure 1a). The 8-arm PEG (100 g in a 500 mL round-bottom flask) was dried by heating with stirring at 85 °C under vacuum [0.06 mm of mercury (8.0 Pa)] for 4 h. The 8-arm PEG was allowed to cool to room temperature. Thionyl chloride (35 mL, 0.48 mol) was added to the flask, which was equipped with a reflux condenser, and the mixture was heated to 85 °C with stirring under a blanket of nitrogen for 24 h. Excess thionyl chloride was removed by rotary evaporation (bath temperature 40 °C). Two successive 50 mL portions of toluene were added and evaporated under reduced pressure (2 kPa, bath temperature 60 °C) to complete the removal of thionyl chloride. The yield of 8-arm PEG-Cl was 100.9 g (99%) by ^{1}H NMR (see Appendix). The end group conversion was determined to be 99% by acetylation of residual hydroxyl end groups and analysis by ^{1}H NMR as follows. A sample of 8-arm PEG-Cl (0.2 g) was dissolved in a mixture of 0.25 mL of acetic anhydride and 0.35 mL of pyridine and left at ambient temperature overnight. The reaction was quenched by the addition of 5 g of ice. The aqueous layer was extracted with three 3 mL portions of chloroform, and the combined chloroform extracts were washed successively with three 1 mL portions of 20% aqueous sodium bisulfate, two 1 mL portions of saturated aqueous sodium bicarbonate, and 1 mL of water. The chloroform was evaporated under reduced pressure. The residue was dissolved in 2 mL of water, and the resulting cloudy solution was concentrated until clear under reduced pressure to remove residual chloroform. The solution was frozen and lyophilized, and the residue was dissolved in DMSO-d_6 and analyzed by ^{1}H NMR (Appendix).

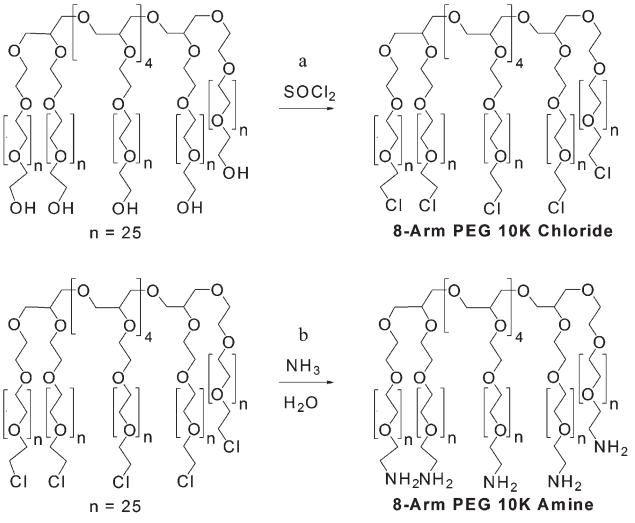

Figure 1. (a) PEG reaction with thionyl chloride to form PEG-chloride and (b) PEG chloride reaction with ammonia to form PEG-amine.

In the second step, 8-arm PEG chloride was converted to 8-arm PEG amine by reaction with aqueous ammonia (Figure 1b). 8-arm PEG-Cl (100.9 g), was dissolved in 640 mL of concentrated aqueous ammonia (28 wt.-%) and heated in a sealed Hastelloy pressure vessel at 60 °C for 48 h. The solution was purged for 1–2 h with dry nitrogen to drive off 50–70 g of ammonia. The solution was then passed through a column (500 mL bed volume) of strongly basic anion exchange resin (Purolite A-860, The Purolite Co., Bala-Cynwyd, PA, USA) in the hydroxide form. The eluent was collected, and three 250 mL portions of deionized water was passed through the column and collected. The aqueous fractions were combined, concentrated under reduced pressure (2 kPa, bath temperature 60 °C) to about 200 g, frozen in portions and lyophilized to give 97.4 g of product (98% yield). Treatment of the 8-arm PEG-NH_2 with excess acetic anhydride in pyridine, and examination of the product in DMSO-d_6 by ^{1}H NMR indicated complete conversion of the chloride end groups and an overall 99% conversion of –OH end groups to –NH_2 end groups (Appendix).

Gelation Time

Equal volumes (100 μL) of dextran aldehyde solution and PEG amine solution were stirred in a 24 well culture plate. The gelation time was defined as the time to form a solid globule, which was completely separated from the bottom of the plate. The results were reported as average and standard deviations of three independent measurements per gel.

Swelling and Degradation

Dextran aldehyde and PEG amine solutions were injected through a dual syringe into a disk shaped rubber mold sandwiched between two glass slides. Disk dimensions were 11 mm in diameter and 3 mm thickness. The swelling was measured at 37 °C by virtue of gravimetric analysis of polymerized disk-shaped PEG/dextran materials in triplicates. Samples were suspended in 100 mL Milli-Q water and weighed prior to hydration and at predetermined time points. The swelling ratio was calculated as follows:

$$\text{Swelling ratio(wt.-\%)} = \frac{W_t - W_d}{W_d} \times 100\% \quad (2)$$

where W_t is the maximal disk mass measured throughout the suspension period and W_d is the initial disk mass prior to suspension (dry sample).

The degradation properties of the materials were extracted from the swelling experiments. The material initially gains weight upon swelling, and the time for the onset of degradation is taken at the point when net weight loss is achieved. Complete degradation occurs when the material completely disintegrates and can no longer be handled or weighed.

Adhesion Strength

Soft tissue adhesion strengths of octyl cyanoacrylate (Dermabond, Ethicon Inc.), fibrin glue (Calbiochem), and PEG/dextran materials

Macromolecular Journals
DOI: 10.1002/mabi.200800355

were compared ex vivo through uniaxial displacements of tissue-material interfaces. Adult Sprague-Dawley rats (300 g, Charles River Laboratories, MA, USA) were sacrificed via carbon dioxide asphyxiation under university IACUC protocol and following federal guidelines for animal care. Following sacrifice, the duodenum of each rat was excised, cleaned, and suspended in Krebs-Henseleit buffer (Sigma, no. k3753) at room temperature. Approximately 2 cm long segments of intestinal tissue were cut and longitudinally bisected along the mesenteric line. Adhesion strength was measured in intestinal segments secured over a tubular fitting with a silicon cuff. This configuration consistently provides stable interactions between the sealants and outer intestinal surfaces, with contact area of 33 mm^2. Intestinal surface samples were attached to the upper and lower arms of a Bose Biodynamic Test Instrument equipped for tensile testing of soft materials. 30 μL adhesive materials were applied directly to the lower intestinal surface. The upper and lower intestinal surfaces were immediately brought into contact, and the adhesive material was allowed to cure onto both tissue surfaces for five minutes under 0.3 N setting force. The tissue-adhesive interface was then displaced at a rate of 0.05 $mm \cdot min^{-1}$ until complete separation. The maximum force measured by the 20 N load cell prior to interface failure was recorded as the adhesion force of the tested material.

Rheological Measurement

Cylindrical PEG/dextran gels were examined in an AR1000N rheometer (TA instruments, New Castle, DE, USA). Rheological measurements were conducted using a parallel 8 mm diameter plate at 37 °C. To avoid slippage at the material plate interface, sand paper (600 grit, ARC abrasives) was added to both plates prior to sample deposition. Shear modulus, *G*, was measured by a creep test across a 2.6 mm gap under 1 N force. Samples were exposed to constant stresses and allowed to recover for 120 s. Strains reached a constant value after 60 s. Moduli of elasticity were determined from stress/strain relationships. The results were reported as average and standard deviations of three measurements per gel.

Scanning Electron Microscopy (SEM)

The morphology of crosslinked PEG/dextran gels was examined by an SEM. Lyophilized gels were fractured after cooling in liquid nitrogen to expose the structure inside the gels. Samples were mounted and sputter coated with gold/palladium using an Anatech LTD Hummer 6.2 sputtering system. The samples were imaged using a JEOL 5600-LV SEM at 10 kV. Changes in pore sizes were estimated using in-house imaging algorithms. Individual pore contours were captured using Adobe Photoshop (Adobe Inc.) from digitized images extracted from the SEM. Each image was subsequently exported to the RGB color space in MATLAB (Mathworks Inc.). The full dynamic range from absolute black (0,0,0) to absolute white (255,255,255) was used. All images were processed with a fixed background of absolute white. For each image, the total number of pixels encompassed by each pore was counted after discarding the pre-defined background in the RGB color space. Total area of each pore was then determined using a standard curve where a single pixel area is 0.11 μm^2.

Proliferation and Cytotoxicity Assays

The *in vitro* cellular response to octyl cyanoacrylate, fibrin glue, and PEG/dextran materials were quantified via colorimetric [3-(4,5-dimethylthiazol-2-yl)-2,5-diphenyltetrazolium bromide (MTT)] assays for cell survival and proliferation (Chemicaon International). Cultures of rat 3T3 fibroblast cells were prepared in 24 well plates using standard techniques. At ≈70% culture confluence, adhesive material treatments were applied using 3 μm pore size well inserts (Falcon). 100 μL of a given adhesive material was polymerized on each well insert followed by introduction into media containing well plates, allowing indirect exposure of cells to test materials and associated by-products. Following material application, cultures were incubated for either 2 or 48 h under standard conditions, followed by immediate analyses of cellular response. MTT assays performed after 2 h treatments indicate the cytotoxic effects of constituent oligomers released to the media due to incomplete polymerization, while 48 h treatment assays reflect the net proliferative effects of polymerization and degradation by-products on target cells. Positive (standard culture treatment) and negative (lysis buffer) controls were performed with both the cytotoxicity and proliferation assays. The cytotoxicity data are converted to relative values by a weighted normalization of MTT absorbance measurements to positive and negative control data, where a value of 0 represents no cytotoxicity and a value of 100 represents maximal cytotoxicity. Proliferation data are converted to percent of control values through normalization of all MTT outputs by the average absorbance of positive control wells.

Statistical Analysis

All data are presented as means ± standard errors. Statistical analyses were performed using one-way ANOVA with post-tests. A *p*-value smaller than 0.05 was considered statistically significant.

Results and Discussion

Dextran aldehyde and 8-arm PEG amine form a crosslinked network with reactive aldehyde groups within minutes when combined as solutions under controlled conditions. In this reaction, aldehyde functional groups within dextran aldehyde react with amino functional groups tethered to 8-arm PEG amine (Figure 2).[23]

Oxidation of the dextran polymer creates multiple aldehyde groups throughout the polymeric chain that enable network crosslinking through formation of imine bonds with the PEG amines and adhesive interaction of the complex material with tissue proteins. The former aldehyde/amine interactions internal to the material provide the cohesive force that solidifies and stabilizes

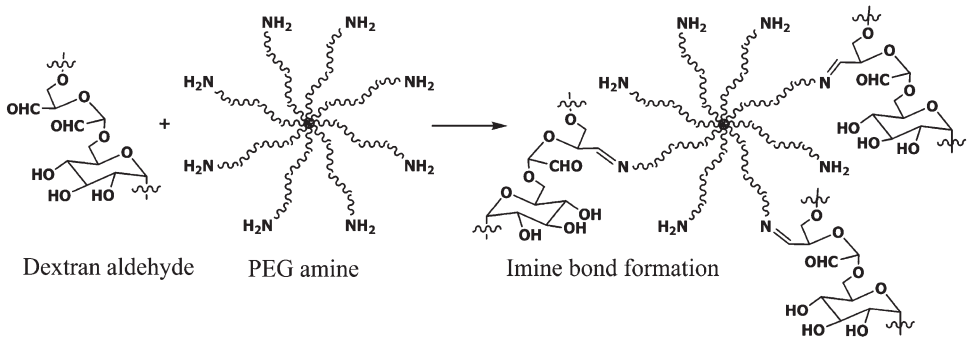

Figure 2. Reaction between dextran aldehyde and PEG amine.

the sealant; the latter external interactions are responsible for material/tissue adhesion. Star PEGs can provide multiple interdigitated targets for the aldehydes[14] and the resultant reticular nature of such an adhesive establishes uniform and dense crosslinking. Control over the amount of oxidized aldehydes and amines regulates material cohesion as well as tissue adhesion which can be tailored to specific tissues as clinical needs dictate.

We examined the effect of changes in structural parameters on gel formation, mechanical properties, adhesion strength, and cytotoxicity. Material compositions were altered with respect to the number of reactive groups present in the constituent polymers; the number of PEG arms (linear or 8-arm PEG) and their associated amine groups; and the dextran oxidation levels which determine the extent of aldehyde groups oxidized from the hydroxyl counterparts. The relative amount of the polymers and their solid content dictate the number of available reactive groups and hence crosslinking density. The following nomenclature is adopted as a means to succinctly denote the compositional parameters (a-f) of a particular material formulation, D(a-*b*-c)P(d-e-f). These represent dextran molecular weight (kDa) (a), dextran oxidative conversion (%) (b), dextran solid content (%) (c), PEG number of arms per molecule (2 or 8) (d), PEG molecular weight of total number of arms (kDa) (e), and PEG solid content (%) (f). Aldehyde to amine ratio denotes the relative amount of aldehydes and amines prior to gel formation which was calculated for each material composition.

Swelling and Degradation: Linear versus Star Gels

To maintain the distance between PEG and dextran reaction points as constant we compared 2 kDa linear and 10 kDa 8-arm PEG. Aldehyde to amine ratios of 1, 3, and 10 were examined for linear and star-PEG based constructs (Figure 3) with respect to their swelling and degradation profile. Linear PEGs do not form gels capable of swelling to a high extent in contrast to star PEGs which extend chemical interactions in multiple directions (Figure 3a). Higher total solid content was used for linear PEG constructs compared to that of the star PEG constructs as lower solid contents of linear PEGs that match those of the star PEG disintegrate quickly and cannot be measured. Even at the higher solid contents linear PEG compositions created gels that disintegrate within several hours (Figure 3b). The high stability achieved for the star PEG constructs compared to linear PEGs results from the formation of highly crosslinked network owing to the larger number of amines available to form imine bonding (Figure 3b). Since 8-arm PEG-based systems remain functional for weeks unlike the linear PEGs, we have focused on star PEG materials. We examined the effects of altering either aldehyde to amine ratio (Figure 4) or total solid content (Figure 5) on gel swelling and degradation profile. For a fixed total solid content, threefold excess in the number of aldehydes compared to amines delayed degradation even in the face of high swelling (Figure 4). This dissonance between swelling and degradation may stem from different efficiencies in network formation when altering aldehyde to amine ratio. As the process of crosslinking becomes more efficient and additional polymer chains are incorporated into the network, the network can withstand the increased swelling. The resulting higher number of chemical bonds in the network leads to a relatively protracted degradation as more bonds need to be hydrolyzed compared to a network having lower crosslinking density.

In our multifunctional system, where dextran oxidation enables multiple aldehyde groups to reside within one polymeric chain and star PEG introduces eight amine groups to one molecule, an equal stoichiometric ratio of aldehydes to amines may not maximize reaction yield as steric interference impedes reaction between these functional groups. The eight functional amine groups in star PEG may not be equally accessible to aldehyde groups in dextran. One can alter the relative amount of functional groups, to control material stability and mechanical properties to create a series of materials with predictable network properties.

Changes in solid content at a fixed aldehyde to amine ratio altered the material swelling kinetics and structure (Figure 5). The higher the solid content, the greater the swelling and the greater the long term integrity of the material. As additional polymeric chains are involved in network formation and more bonds need to be hydrolyzed prior to material disintegration at the higher solid content

Macromol. Biosci. **2009**, *9*, 754–765

Macromolecular Journals
DOI: 10.1002/mabi.200800355

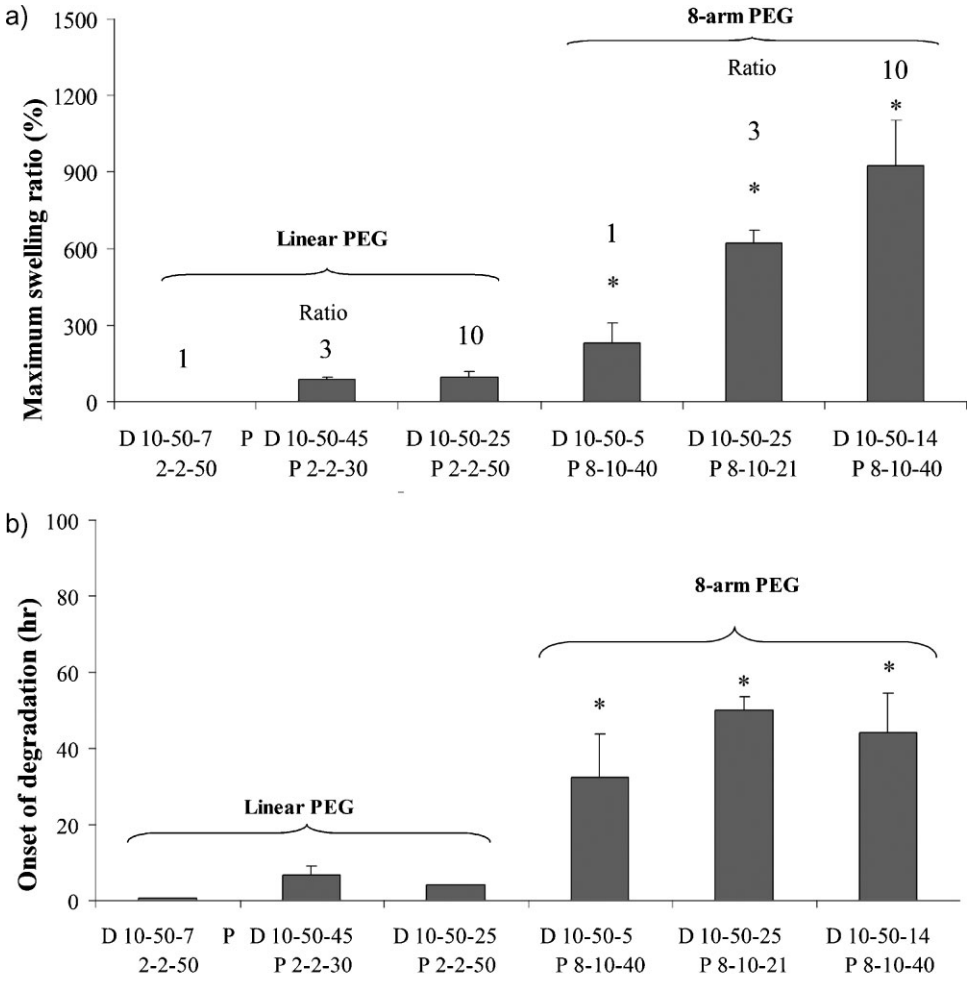

Figure 3. Maximum swelling (a) and onset of degradation (b) for 2 and 8-arm PEG. 8-arm PEG-based materials swell more, and yet present delayed degradation compared to their linear counterparts. All comparisons between 8-arm PEGs and linear PEGs at the same ratio are statistically different ($p < 0.05$).

material, this material can swell more and degrade more slowly. Interestingly, the morphological characteristics of the material are affected by the swelling capacity, as the material that swells more has larger internal pores compared to those in the material that swells less (Figure 5b). Unlike cyanoacrylate and fibrin glue, hydrogel-based materials absorb fluids and swell. This swelling of PEG/dextran is of great potential benefit especially in anastomoses where tight seals are required to limit leakage. The ability to absorb fluids might be at the expense of deterioration in material mechanical properties and adhesion strength, and this feature should be considered in advanced stages of material development.

Gelation and Rheology

Variation in material design parameters imparted an order of magnitude range in gelation time and moduli (Table 1). Increasing PEG or dextran solid content should lower curing times and increase material stiffness, as higher concentrations increase the probability of chemical interactions and a network is formed more efficiently. The same trend is expected for higher dextran oxidation which increases the number of aldehyde groups available for reaction with amines. However, this was not the case when dextran solid content rose from 20 to 40%; gelation time in fact rose only slightly. The increase in time to gel formation and decrease in material stiffness by doubling the aldehyde to amine ratio with doubling of solid content may reflect a dilution effect imparted by excess dextran aldehydes. An excess in one of the polymeric components lowers crosslinking density, giving rise to slower gelation and lower stiffness. This suggests that the extent and kinetics of network formation approach saturation at critical concentrations of constituent dextran aldehyde. We are able to design materials that can be easily applied, and can gel within a clinically relevant time. Optimal materials cure slow enough to be manipulated and fast

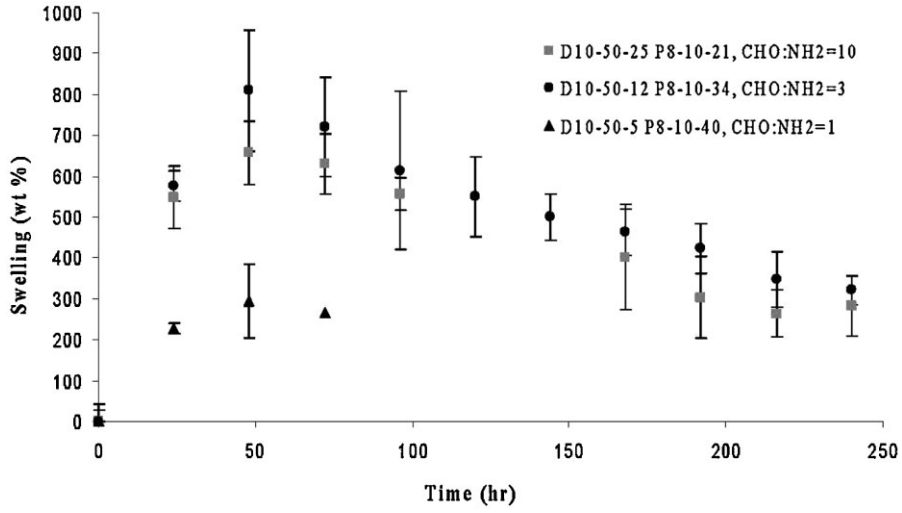

Figure 4. Aldehyde to amine ratio affects swelling and degradation of the materials. There is a ratio in which maximum swelling is accompanied with slow degradation. It is plausible that excess in one of the components act as a diluent, which results in faster degradation as less crosslinking points exist.

enough to be localized in place. Similarly, the ability to control stiffness allows for the selection of material whose mechanical properties match those of a target tissue. This in turn minimizes the potential for tissue damage owing to mechanical mismatch at the tissue/material interface.

Material Adhesion to Rat Small Intestine

PEG/dextran formulations differing in the amount of aldehydes were examined with respect to their adhesion strength to rat small intestine (Figure 6) and compared with adhesion strength of fibrin glue and cyanoacrylate.

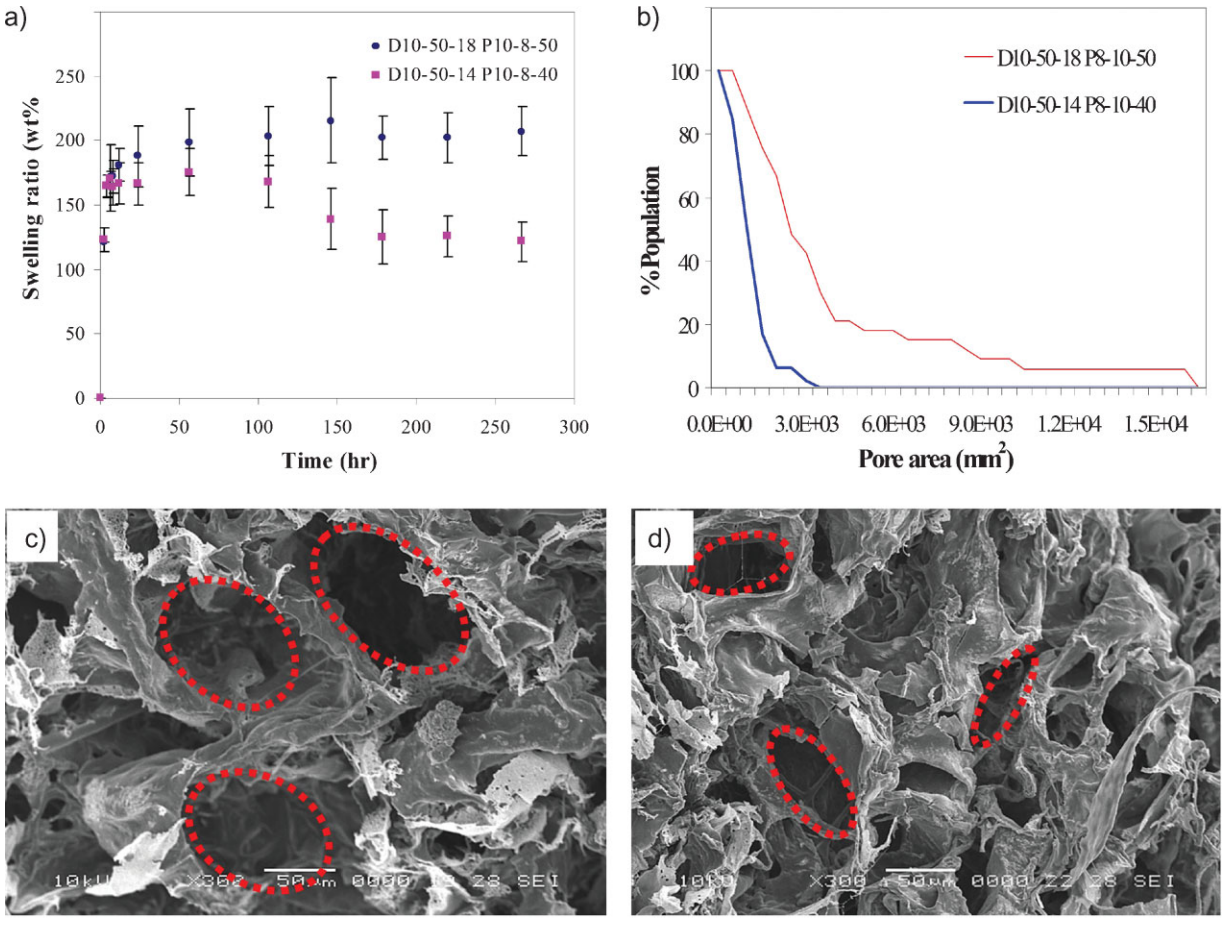

Figure 5. Swelling and degradation of D10-50-14 P8-10-40 and D10-50-18 P8-10-50 (a) and pore areas of these materials estimated by an in-house imaging algorithms using the SEM micrographs (b), as well as SEM of the swollen gels after 24 h in 2 mL PBS at 37 °C for D10-50-18 P8-10-50 (c) and D10-50-14 P8-10-40 (d), bar = 50 μm.

Macromol. Biosci. **2009**, *9*, 754–765

DOI: 10.1002/mabi.200800355

Table 1. Gelation times and moduli for different material variations.

Material	CHO/NH_2	Variable	Gelation time	G'
			s	Pa
D10-20-20 P8-10-60	1	PEG solid content	13 ± 2	81 587 ± 7 340
D10-20-20 P8-10-20	3		115 ± 5	28 005 ± 4 512
D10-20-20 P8-10-20	3	Dextran solid content	115 ± 5	28 005 ± 4 512
D10-20-40 P8-10-20	6		136 ± 16	15 147 ± 2 633
D10-20-20 P8-10-20	3	Dextran oxidation	107 ± 12	28 000 ± 4 512
D10-50-20 P8-10-20	8		30 ± 1	54 380 ± 2 440
D10-50-25 P8-10-21	10	CHO/NH_2 ratio	13 ± 3	54 386 ± 2 440
D10-50-14 P8-10-40	3		10 ± 1	130 558 ± 20 137
D10-50-5 P8-10-40	1		31 ± 4	24 545 ± 4 155

PEG/dextran adhesive strength is bracketed by those of cyanoacrylate and fibrin. Adhesion strength depends on the amount of aldehyde groups which is controlled by altering the dextran aldehyde solid content. PEG/dextran adhesion strength increases and eventually reaches saturation with increasing aldehyde content (Figure 6). This saturation is characterized by a threshold of 20 wt.-% dextran aldehyde solid content. Saturation can result from impregnating the amine groups in the tissue with no additional reaction when more aldehyde groups are presented by the material. Because PEG/dextran materials adhere to tissue through the interaction between aldehyde groups in the adhesive and amine groups in tissues, controlled modulation of aldehyde groups can be matched to tissue amine density. In this way they provide for tissue specific adhesion. This effect links function and biocompatibility. It also contrasts the less specific effects that can cause excessive adhesion as in the case of cyanoacrylate and loose and inadequate adhesion in the case of fibrin.

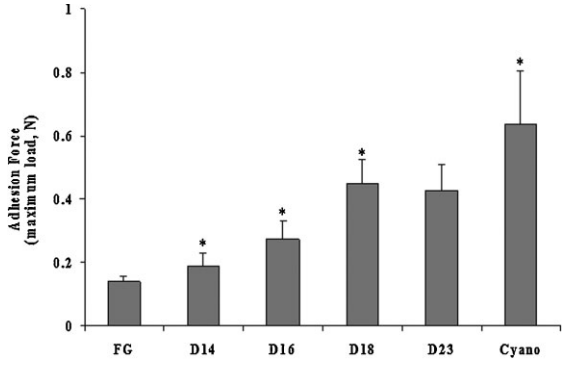

Figure 6. Average adhesion force ($n = 4$) to intestinal tissue of PEG/dextran based adhesive is mediated by the amount of aldehyde groups within the gel and reaches saturation at dextran aldehyde solid contents of about 20 wt.-%. (octylcyanoacrylate denoted as *O*-cyano, fibrin glue as FG and D10, D14, D18, and D23 represent material compositions differing in dextran solid content (D10-50-14, 16, 18 or 23, and P8-10-25). * all samples are statistically different from cyanoacrylate, $p < 0.05$.

Cytotoxicity and Proliferation Assays

A subset of materials which vary in dextran molecular weight was chosen from a larger set of materials to demonstrate the effects on cytotoxicity and proliferation. Since, linear aldehyde-based tissue fixatives, e.g., formaldehyde and glutaraldehyde are tissue toxic,[12] and aldehydes linked to higher molecular weight polymers more biocompatible,[27] we examined the effect of dextran molecular weight on cytotoxicity. The relative cytotoxicity values of the tested PEG/dextran formulations were

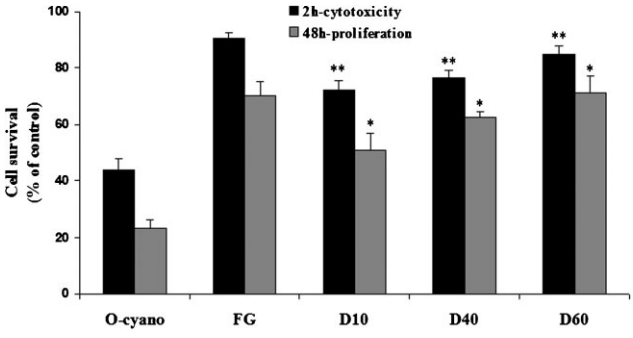

Figure 7. Cytotoxicity and proliferation of octyl-cyanoacrylate, fibrin sealant, and PEG/dextran materials using fibroblast are depicted. PEG/dextran-based adhesive presents less than half of relative cytotoxicity compared to cyanoacrylate. The higher the dextran molecular weight is, the more limited are the mobility and cellular penetration capacity, and the higher the proliferation is (octylcyanoacrylate denoted as *O*-cyano, fibrin glue as FG and D10, D40, and D60 represent material compositions differing in dextran molecular weight (D10-21-21 P8-10-25, D40-25-18 P8-10-25, and D60-23-20 P8-10-25). *, ** samples are statistically different from cyanoacrylate and fibrin glue, $p < 0.05$.

bracketed by those of cyanoacrylate and fibrin treatments, with an inverse dependence on constituent dextran aldehyde molecular weight. Increasing dextran aldehyde molecular weight results in higher cell survival at 2 h, and higher fibroblasts proliferation at 48 h (Figure 7). The reduction in cytotoxicity with an increased dextran molecular weight is explainable in terms of the cellular uptake of material by-products (PEG or dextran chains), as larger constituent molecules typically reduce polymer by-product reactivity with cells.[28]

There may well be a trade-off between adhesion, tissue compatibility, and compositional control of materials. However, in the case of PEG/dextran sealants both adhesion and biocompatibility can be improved at the same time. Up to a certain range, higher dextran aldehyde solid content improve adhesion strength (Figure 6) while lower cytotoxicity and higher proliferation can be imparted by controlling dextran molecular weight (Figure 7).

Conclusion

The limitations of commercially available sealants have raised the need for the development of a material that can be mediated to control both adhesion strength and biocompatibility while maintaining material cohesive properties throughout the time the material is clinically needed. Adhesive sealants based on aminated star polyethylene glycol and dextran aldehyde polymers (PEG/dextran) have the potential for biocompatible adhesion. By melding two polymers, PEG and dextran that control material cohesive properties and adhesive properties, respectively, one can create a modulated set of adhesive materials for specific applications ranging in their physicochemical properties, degradation time, adhesion strength and biocompatibility. Possibility emerges to modify materials for specific tissues to adhere in a tissue-dependent mode. Follow up studies will focus on examining adhesion of PEG/dextran materials to different tissues and matching tissue-material properties.

Appendix

^{1}H NMR of P8-10-1-Cl

^{1}H NMR was utilized to calculate residual hydroxyl groups in the PEG amine synthesis. For each of the two steps of the synthesis reaction, PEG chloride and PEG amine and their acetylated products were scanned using ^{1}H NMR. The

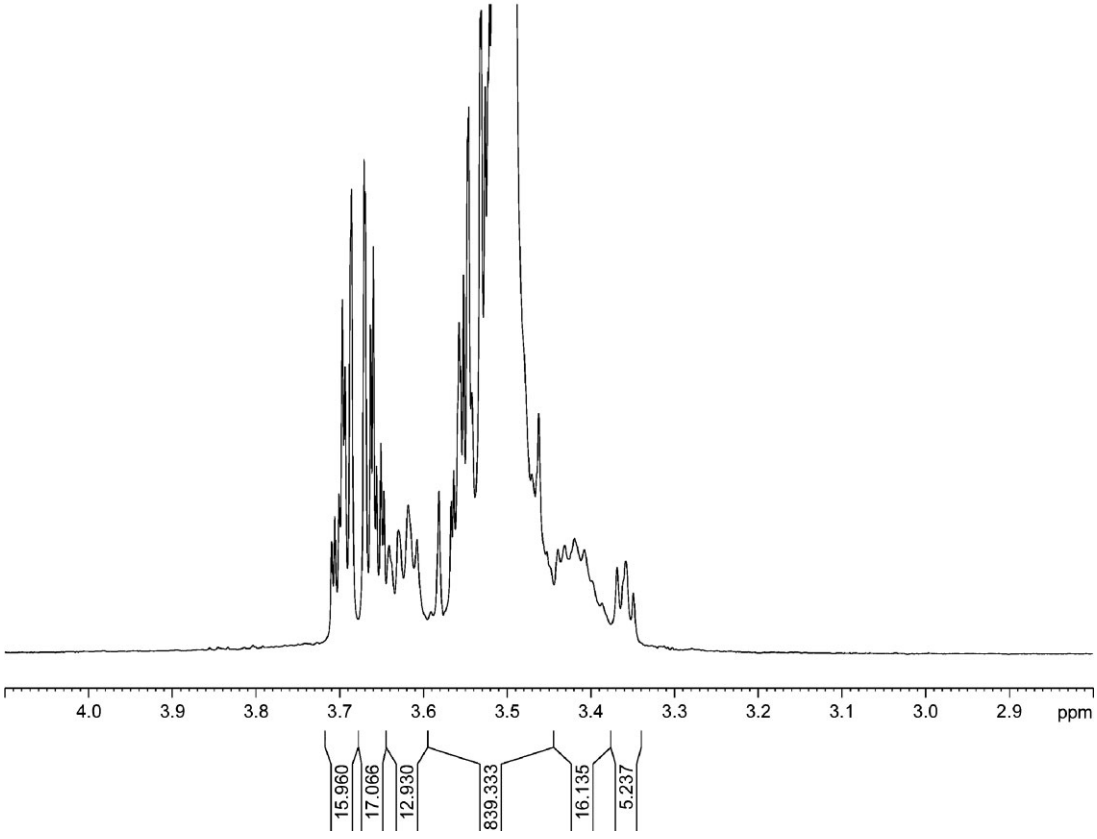

Figure A1. ^{1}H NMR of PEG chloride showing a peak at $\delta = 3.72–3.68$ (m, 2H, CH_2Cl).

Macromol. Biosci. **2009**, *9*, 754–765

DOI: 10.1002/mabi.200800355

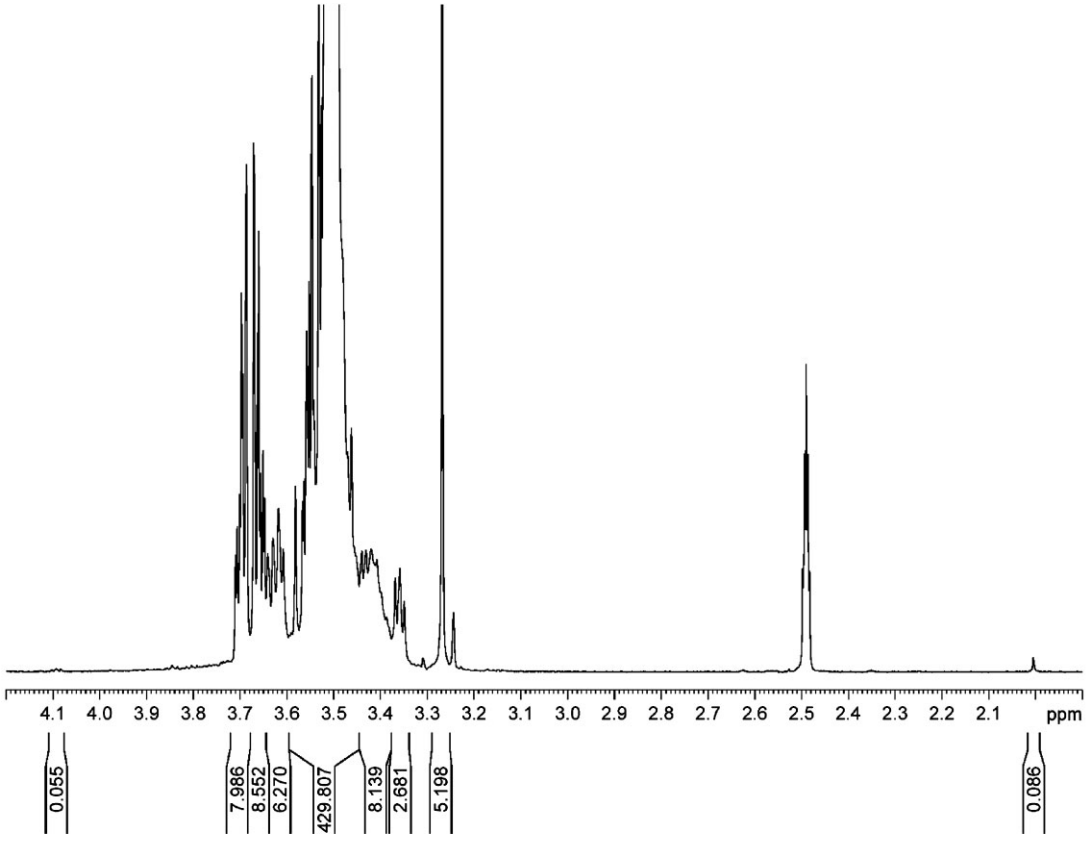

Figure A2. ^{1}H NMR of acetylated PEG chloride showing peaks at $\delta = 4.09$ (t, $J = 4.7$ Hz, 2H, C$\underline{H}_2$OAc), 3.72–3.68 (m, 2H, CH_2Cl), and 2.00 (s, 3H, AcO).

proportion of residual hydroxyl end groups in the 8-arm PEG-Cl was determined by comparing the integrals of the ^{1}H NMR peaks for the CH_2Cl end groups [$\delta = 3.72$–3.68 (m, 2H, CH_2Cl)] with that of the $-CH_2OAc$ end groups [$\delta = 4.09$ (t, $J = 4.7$ Hz, 2H, C$\underline{H}_2$OAc) and 2.00 (s, 3H, AcO)] (Figure A2).

Acetylation Analysis of P8-10-1-Cl

To calculate overall end group conversion we compared the integrals of peaks at $\delta = 4.09$ (t, $J = 4.7$ Hz, 2H, CH_2OAc) and 2.00 (s, 3H, AcO) with peaks at $\delta = 3.72$–3.68 (m, 2H, CH_2Cl) according to

$$\%\ \text{conversion} = \frac{(\int 3.72 - 3.68)/2}{(\int 3.72 - 3.68)/2 + (\int 4.09 + \int 2.00)/5} \times 100\% \quad (1)$$

where $\int$3.72–3.68 denotes the integral of the peak at $\delta = 3.72$–3.68, $\int$4.09 the integral of the peak at $\delta = 4.09$, etc.

In the acetylation analysis of P8-10-1-Cl above,

$$\%\ \text{conversion} = \frac{7.986/2}{7.986/2 + (0.055 + 0.086)/5} \times 100\% = 99\%$$

^{1}H NMR of P8-10-1-NH_2

The proportion of residual hydroxyl end groups in the 8-arm PEG-NH_2 was determined by comparing the integrals of the ^{1}H NMR peaks for the $-CH_2OAc$ end groups [$\delta = 4.09$ (t, $J = 4.7$ Hz, 2H, CH_2OAc) and 2.00 (s, 3H, AcO)] with those of the $-CH_2NHAc$ end groups [$\delta = 3.16$ (q, $J = 5.8$ Hz, 2H, CH_2N) and 1.78 (s, 3H, AcN)] (Figure A4).

Acetylation Analysis of P8-10-1-NH_2

To calculate overall end group conversion, we compared the integrals of peaks at $\delta = 4.09$ (t, $J = 4.7$ Hz, 2H, C$\underline{H}_2$OAc) and 2.00 (s, 3H, AcO) with those of peaks at $\delta = 3.16$ (q,

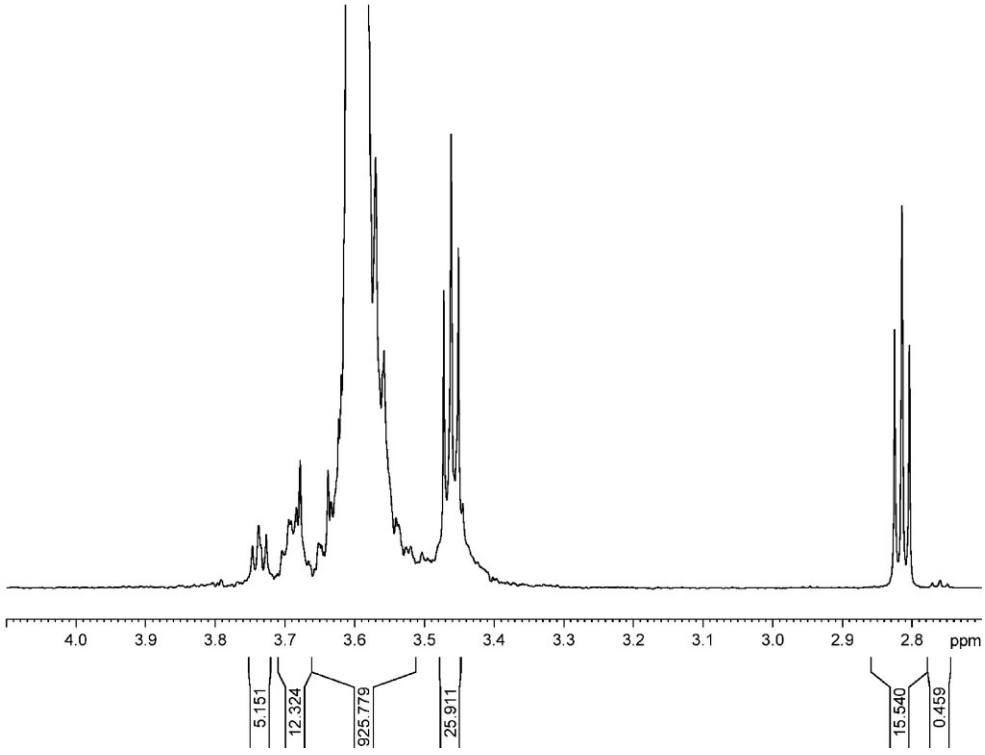

Figure A3. ^{1}H NMR of PEG amine showing a peak at $\delta = 2.81$ (t, $J = 5.2$ Hz, 2H, $-CH_2NH_2$).

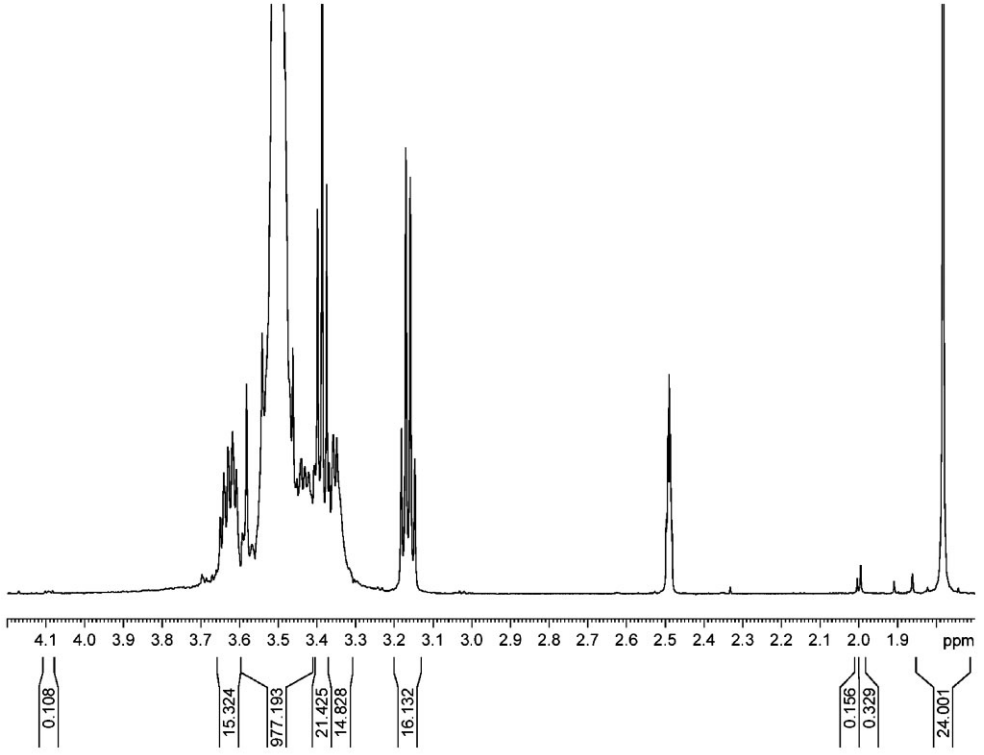

Figure A4. ^{1}H NMR of acetylated PEG amine showing peaks at $\delta = 4.09$ (t, $J = 4.7$ Hz, 2H, CH_2OAc), 3.16 (q, $J = 5.8$ Hz, 2H, CH_2N), $\delta = 2.00$ (s, 3H, AcO) and 1.78 (s, 3H, AcN).

Macromol. Biosci. **2009**, *9*, 754–765

DOI: 10.1002/mabi.200800355

$J = 5.8$ Hz, 2H, CH_2N), 1.78 (s, 3H, AcN) according to

$$\% \text{ conversion} = \frac{(\int 3.16 + \int 1.78)/5}{(\int 3.16 + \int 1.78)/5 + (\int 4.09 + \int 2.00)/5} \times 100\% \quad (2)$$

where $\int 3.16$ is the integral of the peak at $\delta = 3.16$, etc.

In the acetylation analysis above,

$$\% \text{ conversion} = \frac{(16.132 + 24.001)/5}{(16.132 + 24.001)/5 + (0.108 + 0.156)/5} \times 100\% = 99\%$$

Acknowledgements: The authors acknowledge *DuPont* for financial support and productive collaboration in this research. Much appreciation goes to Dr. *Samuel Arthur* from DuPont for providing dextran aldehydes and PEG amines. The authors would like to thank Dr. *Vijaya Kolachalama* for the analysis of the SEM images.

Received: December 12, 2008; Revised: January 27, 2009; Accepted: January 28, 2009; DOI: 10.1002/mabi.200800355

Keywords: adhesives; dextran; hydrogels; PEG; tissue

[1] A. Akgun, S. Kuru, C. Uraldi, O. Tekin, B. Karip, T. Tug, A. U. Ongoren, *Tech. Coloproctol.* **2006**, *10*, 208.
[2] M. Araki, H. Tao, N. Nakajima, H. Sugai, T. Sato, S. H. Hyon, T. Nagayasu, T. Nakamura, *J. Thorac. Cardiovasc. Surg.* **2007**, *134*, 1241.
[3] M. G. Lee, D. Jones, *Surg. Innov.* **2005**, *12*, 203.
[4] J. R. Salameh, J. H. Schwartz, D. A. Hildebrandt, *Am. J. Surg.* **2006**, *191*, 791.
[5] O. Saygun, S. Topaloglu, F. M. Avsar, H. Ozel, S. Hucumenoglu, M. Sahin, S. Hengirmen, *Can. J. Surg.* **2006**, *49*, 107.
[6] D. J. Byrne, J. Hardy, R. A. Wood, R. McIntosh, D. Hopwood, A. Cuschieri, *J. R. Colloid Surg. Edinb.* **1992**, *37*, 394.
[7] J. Figueras, L. Llado, M. Miro, E. Ramos, J. Torras, J. Fabregat, T. Serrano, *Ann. Surg.* **2007**, *245*, 536.
[8] T. Lamsa, H. T. Jin, J. Sand, I. Nordback, *Pancreas* **2008**, *36*, 261.
[9] P. A. Leggat, D. R. Smith, U. Kedjarune, *ANZ. J. Surg.* **2007**, *77*, 209.
[10] D. Hopwood, *Histochemie* **1969**, *17*, 151.
[11] H. Hata, H. Takano, G. Matsumiya, N. Fukushima, N. Kawaguchi, Y. Sawa, *Ann. Thorac. Surg.* **2007**, *83*, 1621.
[12] M. B. St Clair, E. Bermudez, E. A. Gross, B. E. Butterworth, L. Recio, *Environ. Mol. Mutagen.* **1991**, *18*, 113.
[13] H. W. Sung, D. M. Huang, W. H. Chang, R. N. Huang, J. C. Hsu, *J. Biomed. Mater. Res.* **1999**, *46*, 520.
[14] US 2007249870 (2006), inv.: H. K. Chenault.
[15] J. A. Cadee, M. J. van Luyn, L. A. Brouwer, J. A. Plantinga, P. B. van Wachem, C. J. de Groot, W. den Otter, W. E. Hennink, *J. Biomed. Mater. Res.* **2000**, *50*, 397.
[16] B. Baroli, *J. Chem. Technol. Biotechnol.* **2006**, *81*, 491.
[17] W. S. Koegler, L. G. Griffith, *Biomaterials* **2004**, *25*, 2819.
[18] N. A. Peppas, K. B. Keys, M. Torres-Lugo, A. M. Lowman, *J. Controlled Release* **1999**, *62*, 81.
[19] J. Lleixa Calvet, D. Grafahrend, D. Klee, M. Moller, *J. Mater. Sci.: Mater. Med.* **2008**, *19*, 1631.
[20] A. S. Sawhney, C. P. Pathak, J. J. van Rensburg, R. C. Dunn, J. A. Hubbell, *J. Biomed. Mater. Res.* **1994**, *28*, 831.
[21] B. P. Lee, J. L. Dalsin, P. B. Messersmith, *Biomacromolecules* **2002**, *3*, 1038.
[22] P. Caliceti, F. M. Veronese, *Adv. Drug Deliv. Rev.* **2003**, *55*, 1261.
[23] S. K. Bhatia, S. D. Arthur, H. K. Chenault, G. K. Kodokian, *Biotechnol. Lett.* **2007**, *29*, 1645.
[24] T. M. Shazly, N. Artzi, F. Boehning, E. R. Edelman, *Biomaterials* **2008**, *29*, 4584.
[25] S. K. Bhatia, S. D. Arthur, H. K. Chenault, G. D. Figuly, G. K. Kodokian, *Curr. Eye Res.* **2007**, *32*, 1045.
[26] US 2006078536 (2006), inv.: G. K. A. Kodokian, S. David.
[27] J. R. Kuykendall, M. S. Bogdanffy, *Mutat. Res.* **1992**, *283*, 131.
[28] D. M. Toriumi, W. F. Raslan, M. Friedman, M. E. Tardy, *Arch. Otolaryngol. Head Neck Surg.* **1990**, *116*, 546.